ARTICLE

Preparation and isolation of mono-Nb substituted Keggin-type phosphomolybdic acid and its application as an oxidation catalyst for isobutylaldehyde and Wacker-type oxidation

Received 00th January 20xx,
Accepted 00th January 20xx

DOI: 10.1039/x0xx00000x

Takashi Matono,[a] Shinsuke Ueno,[a] Yuki Kato,[b] Naoya Umehara,[a] Zhongling Lang,[c] Yangguang Li,[c] Wataru Ninomiya,[b] Maher El Hallal,[d] Edgar Osiris Yanes Gonzales-Yañez,[d] Mickael Capron,[d] Satoshi Ishikawa,[e] Wataru Ueda,[e] Tsuneji Sano[a] and Masahiro Sadakane*[a]

Potassium and proton mixed salt of mono-Nb substituted Keggin-type phosphomolybdate, $KH_3[PMo_{11}NbO_{40}]$, was isolated in pure form by reacting Keggin-type phosphomolybdic acid ($H_3[PMo_{12}O_{40}]$) and potassium hexaniobate ($K_8Nb_6O_{19}$) in water, followed by freeze-drying. The all protonic form, $H_4[PMo_{11}NbO_{40}]$, was isolated via proton exchange with H-resin and subsequent freeze-drying. The most crucial factor to isolate $KH_3[PMo_{11}NbO_{40}]$ and $H_4[PMo_{11}NbO_{40}]$ in pure form is the evaporation of water using the freeze-drying method. Using a similar procedure, the potassium salt of the di-Nb substituted compound $K_5[PMo_{10}Nb_2O_{40}]$ was isolated. $H_4[PMo_{11}NbO_{40}]$ exhibited high catalytic activity for oxidizing isobutylaldehyde oxidation to methacrolein and moderate catalytic activity for the Wacker-type oxidation of allyl phenyl ether when combined with $Pd(OAc)_2$.

Introduction

Keggin-type heteropolymetalates, $[X^{n+}M_{12}O_{40}]^{(8-n)-}$ (X = P^{5+} or Si^{4+}; M = W^{6+} and/or Mo^{6+}) where one tetrahedral XO_4 is surrounded by 12 octahedral MO_6 (Fig. 1(a) and (b)), are one of the most common family of polyoxometalates. Their acidic forms, so-called heteropolyacids, $H_{8-n}[X^{n+}M_{12}O_{40}]$, exhibit strong acidic and redox properties, and therefore are used as functional materials such as acid catalysts, oxidation catalysts, and buttery materials.[1-4] Their properties can be tuned by substituting W or Mo with other transition metals (Fig. 1(c)).[5] Vanadium-substituted Keggin-type phosphomolybdic acids, $H_{3+x}[PMo_{12-x}V^{5+}{}_xO_{40}]$ (x = 1, 2, 3), are the mostly used heteropolyacids as redox catalysts.[6-9]

Niobium also forms polyoxometalates,[10] and it is well established that Nb can be substituted into W-based Keggin-type heteropolytungstates. Examples include mono-Nb and tri-Nb substituted heteropolytungstates, and substitution of W^{6+}=O with Nb^{5+}=O causes localization of the negative charge on the oxygen atoms around Nb, thus changing the reactivity of heteropolytungstates toward cationic species and organic compounds.[11, 12] Preparation and characterization of the mono-Nb substituted phosphotungstate, $[PW_{11}NbO_{40}]^{4-}$ has been reported by several groups such as Sécheresse et al.,[13] Beer et al.,[14] Okumura et al.,[15] Song et al.,[16] and Abramov et al.[17, 18] The tri-Nb ($Nb_3O_3(=O)_3$) moiety selectively reacts with metal–organic cations and trialcohols.[19, 20] Furthermore, the substituted Nb=O moiety can act as catalytic center for oxidation reaction using H_2O_2.[21, 22]

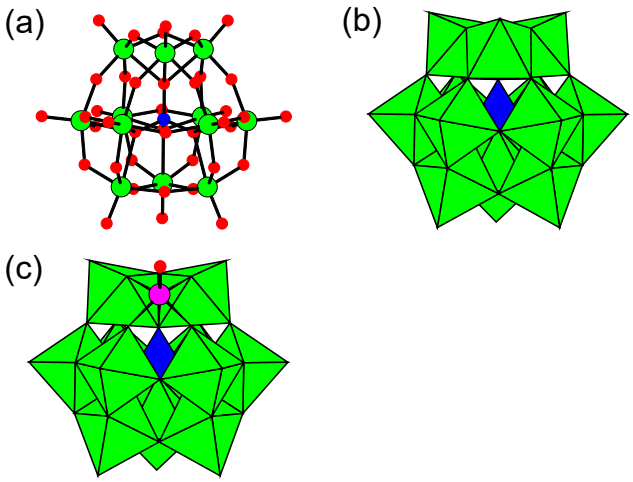

Fig. 1 (a) Ball-and-stick representation and (b) polyhedral representation of Keggin-type heteropolymetalate, and (c) polyhedral representation of mono-metal substituted Keggin-type heteropolymetalate. Blue, green, red, and pink balls represent central X cation (P^{5+} or Si^{4+}), M metal (W^{6+} or Mo^{6+}), oxygen, and substituting metal, respectively. Blue and green polyhedron represents XO_4 and MO_6 polyhedron, respectively.

[a] *Department of Applied Chemistry, Graduate School of Advanced Science and Engineering, Hiroshima University, 1-4-1, Kagamiyama, Higashi-Hiroshima, 739-8527, Japan.*
[b] *MMA R&D Center, Mitsubishi Chemical Corporation, 20-1, Miyuki-cho, Ootake, Hiroshima 739-0693, Japan.*
[c] *Key Laboratory of Polyoxometalate and Reticular Material Chemistry of Ministry of Education, Faculty of Chemistry, Northeast Normal University, Changchun 130024, China.*
[d] *Université de Lille, CNRS, Centrale Lille, ENSCL, Université Artois, UMR 8181 – UCCS – Unité de Catalyse et Chimie du Solide, F-59000 Lille, France.*
[e] *Department of Material and Life Chemistry, Faculty of Engineering, Kanagawa University, 3-27, Rokkakubashi, Kanagawa-ku, Yokohama 221-8686, Japan.*
† Footnotes relating to the title and/or authors should appear here.
Electronic Supplementary Information (ESI) available: [Fig. S1 and S2 ESI-MS, Fig. S3 Simulated IR, Fig. S4, S5 ^{31}P NMR]. See DOI: 10.1039/x0xx00000x

However, there are only few reports on the synthesis of Mo-based Keggin-type phosphomolybates with substituted Nb. There is no preparation method with high purity and clear characterization evidences of mono-Nb substituted phosphomolybdate, $[PMo_{11}NbO_{40}]^{4-}$.

Ressler et al. prepared $H_4[PMo_{11}NbO_{40}]$ via the reaction of $K_8Nb_6O_{19}$, K_2HPO_4, and MoO_3 dissolved by the addition of excess K_2CO_3 followed by acidification with $HClO_4$.[23] The resulting solid was analyzed by X-ray absorption fine structure (XAFS) spectroscopy and thermogravimetry differential thermal analysis (TG-DTA). Davis et al. prepared $[PMo_{11}NbO_{40}]^{4-}$ by a reaction of *in-situ* prepared $[PMo_{11}O_{39}]^{7-}$ with Nb oxalate.[24, 25] In both cases, no clear evidence of the molecular structure of $[PMo_{11}NbO_{40}]^{4-}$ by ^{31}P Nuclear magnetic resonance (NMR), Infrared (IR) and electrospray ionization mass spectrometry (ESI-MS) has been reported. Abramov et al. reported the formation of $[PMo_{12-x}Nb^{5+}{}_xO_{40}]^{(3+x)-}$ by mixing a Keggin-type phosphomolybdic acid, $H_3[PMo_{12}O_{40}]$, and ammonium niobium oxalate, $(NH_4)[NbO(C_2O_4)_2(H_2O)]$, in aqueous solutions.[26] The desired species were detected by high-performance liquid chromatography-inductively coupled plasma (HPLC-ICP) mass spectrometry and ^{31}P NMR; however, these isolated molecules were mixed with other species and no isolation has been reported. Weinstock et al. reported the preparation of a di-Nb substituted Keggin-type phosphomolybdate, $[PMo_{10}Nb_2O_{40}]^{5-}$, with full characterization and polymerization reactions through the Nb-O-Nb bonds.[27]

Here, we report the isolation of potassium salts of mono- and di-Nb substituted phosphomolybdates, $H_3K[PMo_{11}NbO_{40}]$ and $K_5[PMo_{10}Nb_2O_{40}]$, respectively, in pure form by reacting $H_3[PMo_{12}O_{40}]$ and $K_8Nb_6O_{19}$. The full protonic form of the mono-Nb substituted compound, $H_4[PMo_{11}NbO_{40}]$, was also isolated in high purity, whereas the di-Nb species were not stable under acidic conditions. We also report that the catalytic performances for the oxidative dehydrogenation of isobutylaldehyde to methacrolein of the $H_4[PMo_{11}NbO_{40}]$ are higher than those of $H_4[PMo_{11}VO_{40}]$ and $H_3[PMo_{12}O_{40}]$, and $H_4[PMo_{11}NbO_{40}]$ shows moderate catalytic activity for the Wacker-type oxidation of allyl phenyl ether.

Experimental

Materials and methods

Reagents and materials.

Ammonium niobium oxalate, $(NH_4)[NbO(C_2O_4)_2(H_2O)]$-$nH_2O$, was obtained from the Japan Reference Catalyst (JRC-NBO-3AO) of the Catalysis Society of Japan, and the amount of hydrate was estimated using TG-DTA. Phosphomolybdic acid, $H_3[PMo_{12}O_{40}]$-$29.4H_2O$, silicomolybdic acid, $H_4[SiMo_{12}O_{40}]$-nH_2O, phosphomolybdovanadic acid, $H_4[PMo_{11}VO_{40}]$-nH_2O, were obtained from Nippon Inorganic Colour & Chemical. Co., Ltd and amount of hydrate was estimated by TG-DTA. $K_8Nb_6O_{19}$ was obtained from Mitsuwa Chemicals Co., Ltd., and the amount of water in $K_8Nb_6O_{19}$-$16.6H_2O$ was estimated by TG-DTA. All other chemicals were of reagent grade and were used without further purification.

Preparation of $H_3K[PMo_{11}NbO_{40}]$-$4H_2O$

$K_8Nb_6O_{19}$-$16.6H_2O$ (0.373 g, Nb 1.5 mmol) dissolved in H_2O (5.0 mL) was added to an aqueous solution of $H_3PMo_{12}O_{40}$-$29.4H_2O$ (3.532 g, 1.5 mmol) dissolved in H_2O (5.0 mL). After the mixture was stirred at 85 °C for 3 h in a closed glass reactor, the produced yellow precipitates were removed by centrifugation (11000 rpm, 12851 RCF ×G, KOKUSAN) for 20 min. The clear yellow solution was freeze-dried (FDU-2200, EYEA) to form yellow solid (~1.50 g, mmol, 51.7 % based on P).

Elem. Anal. Calcd for $H_3K[PMo_{11}NbO_{40}]$-$4H_2O$: H, 0.6; P, 1.6; Mo, 54.6; Nb: 4.8; K, 2.0. Found: H, 0.9; P, 1.6; Mo, 54.8; Nb: 4.7; K, 2.0.

Preparation of $H_4[PMo_{11}NbO_{40}]$-$11H_2O$

$K_8Nb_6O_{19}$-$16.6H_2O$ (0.373 g, Nb 1.5 mmol) dissolved in H_2O (5.0 mL) was added to an aqueous solution of $H_3PMo_{12}O_{40}$-$29.4H_2O$ (3.532 g, 1.5 mmol) dissolved in H_2O (5.0 mL). After the mixture was stirred at 85 °C for 3 h in a closed glass reactor, the produced yellow precipitates were removed by centrifugation (11000 rpm, 12851 RCF ×G, KOKUSAN) for 20 min. The clear light-yellow solution was passed through H-resin (Dowex-50W, 5.0 g), and the yellow eluent was freeze-dried (FDU-2200, EYEA) to form a yellow solid (1.30 g, mmol, 45.3 % based on P).

Elem. Anal. Calcd for $H_4[PMo_{11}NbO_{40}]$-$11H_2O$: P, 1.5; Mo, 52.2; Nb: 4.6; K, 0.0. Found: P, 1.5; Mo, 52.3; Nb: 4.6; K, 0.0.

Preparation of $K_5[PMo_{10}Nb_2O_{40}]$-$16H_2O$

$K_8Nb_6O_{19}$-$16.6H_2O$ (0.4977 g, Nb 1.98 mmol) dissolved in H_2O (2.5 mL) was added to an aqueous solution of $H_3PMo_{12}O_{40}$-$29.4H_2O$ (1.1775 g, 0.5 mmol) dissolved in H_2O (2.5 mL). After the mixture was stirred at 85 °C for 3 h in a closed glass reactor, the produced yellow precipitates were removed by centrifugation (11000 rpm, 12851 RCF ×G, KOKUSAN) for 20 min. The clear yellow solution was freeze-dried (FDU-2200, EYEA) to form yellow solid (~ 0.445 g, mmol, 35.2 % based on P).

Elem. Anal. Calcd for $K_5[PMo_{10}Nb_2O_{40}]$-$16H_2O$: P, 1.3; Mo, 41.7; Nb: 8.1; K, 8.5; H, 1.4. Found: P, 1.3; Mo, 41.6; Nb: 8.0; K, 8.7; H, 0.9.

Other analytical techniques

IR spectra were recorded on a NICOLET 6700 FT-IR spectrometer (Thermo Fisher Scientific) using KBr pellets. ^{31}P NMR spectra were recorded on a Varian system 500 (500 MHz) spectrometer (Agilent) (P resonance frequency: 202.378 MHz). The spectra were referenced with an external 85 % H_3PO_4 (0 ppm). Elemental analyse were performed at the Analysis Center of Mitsubishi Chemical Co. (Ootake, Japan). High-resolution ESI-MS spectra were recorded using an LTQ Orbitrap XL instrument (Thermo Fisher Scientific) with an accuracy of 3 ppm. Each sample (5 mg) was dissolved in 5 mL of H_2O, and the solutions were diluted with CH_3CN (final concentration: ~10 μg/mL). TG-DTA was measured using TG/DTA7300 (SII, Japan) under N_2 flow of 50 mL·s^{-1}.

Computational details

Geometry optimization and vibrational frequency calculations were performed for two polyoxometalate species, $[PMo_{12}O_{40}]^{3-}$ and $[PMo_{11}NbO_{40}]^{4-}$, using the B3LYP functional.[28, 29] All the calculations were performed using the Gaussian09 package (revision D.01).[30] For the main groups of O and P atoms, the 6-

31+G* atomic basis set was used,[31, 32] and for the transition-metal Mo and Nb atoms, the SDD basis set was employed.[33-36]

Evaluation of catalytic performance

Oxidation of iso-butylaldehyde

Phosphomolybdic acid compounds were pressed into pellets and crushed. The crushed powders were sieved through two sieves to obtain a particle size of 0.25–0.5 mm. The catalysts (0.3–2.5 g) were placed into a fixed-bed continuous flow reactor under atmospheric pressure at 240 °C. The reactions were carried out under total flow rate 9 L/h of reactant gas, which consist of $P(i\text{-}C_4H_8O)$ = 1.4 kPa, $P(O_2)$ = 10.1 kPa, $P(H_2O)$ = 10.3 kPa and $P(N_2)$ = 78.5 kPa, as partial pressure. Amount of isobutylaldehyde was calculated using 22.4 dm^3/mol at 0 °C under 1013 hPa. Reactions without catalysts were performed under the same conditions, where isobutylaldehyde conversion and selectivity to methacrolein were 4.3% and 12.0%, respectively. Reactions without catalysts have also been reported.[37] The reaction products were analyzed by gas chromatography (GC) with Thermal conductivity detector (TCD) and Flame ionization detector (FID). The columns in GC with TCD detector and Molecular Sieve 5 A (0.3 m ×Φ 3 mm) were used for the detection of CO and O_2 and Porapak Q column (2 mm × Φ 3 mm) was employed for the detection of CO_2. The GC column with the FID detector was DB-FFAP (30 m×Φ 0.32 mm) capillary column used for the detection of isobutylaldehyde and methacrolein.

Wacker-type oxidation of allyl phenyl ether

In a glass tube, CH_3CN/H_2O (7/1, v/v, 10 mL) mixed solvent, allyl phenyl ether (1 mmol), biphenyl (0.5 mmol) as an internal standard, $Pd(OAc)_2$ (0.1 mmol), POM (0.03 mmol) were placed and a balloon filled with O_2 gas was attached. The reaction was conducted in an oil bath at 60 °C with stirring. After the reaction, quantification was performed using GC and ^{1}H NMR.

Results and discussion

Synthesis and Isolation of $H_3K[PMo_{11}NbO_{40}]$ and $K_5[PMo_{10}Nb_2O_{40}]$

Abramov et al. reported the synthesis of $[PMo_{11}NbO_{40}]^{4-}$ and $[PMo_{10}Nb_2O_{40}]^{5-}$ by a reaction of $H_3[PMo_{12}O_{40}]$ (7 mM) and $(NH_4)[NbO(C_2O_4)_2(H_2O)]$ in water at 60 °C for 12 h.[26] Characterization using HPLC-ICP, HPLC-UV, and ^{31}P NMR indicated that the products were a mixture of $[PMo_{11}NbO_{40}]^{4-}$, $[PMo_{10}Nb_2O_{40}]^{5-}$, and $[PMo_{12}O_{40}]^{3-}$, and is the first reasonable characterization of Nb-substituted Keggin-type phosphomolybdates using ^{31}P NMR and elemental analysis. Inspired by their pioneer work indicating that Nb=O can substitute Mo=O by mixing Nb source and $H_3[PMo_{12}O_{40}]$, we modified the preparation method and found a preparation method to obtain high-purity $[PMo_{11}NbO_{40}]^{4-}$.

Heating a mixture of $H_3[PMo_{12}O_{40}]$ (150 mM) and potassium hexaniobate, $K_8[Nb_6O_{19}]$ (150 mM of Nb), in water at 85 °C for 3 h produces yellow solution with yellow precipitates which was separated by centrifugation. ^{31}P NMR spectrum of the yellow solution shows a new peak at −2.92 ppm which is different from the chemical shift (−3.20 ppm) of the $H_3[PMo_{12}O_{40}]$ (Fig. 2 (b) and (a)). High-resolution ESI-MS of the solution revealed profiles assignable to $H[PMo_{11}NbO_{40}]^{3-}$ and $[PMo_{11}NbO_{40}]^{4-}$ (Fig. S1). These results indicate that the high-purity compound, $[PMo_{11}NbO_{40}]^{4-}$, was produced in water.

Isolation of the $[PMo_{11}NbO_{40}]^{4-}$ by evaporation of water was performed at different temperatures, and the obtained yellow solids were characterized by ^{31}P NMR after the solids were dissolved in D_2O (Fig. 3). Solids obtained by drying at a temperature more than 40 °C show several ^{31}P NMR signals indicating that the $[PMo_{11}NbO_{40}]^{4-}$ decomposes during the drying process. Conversely, solid obtained by freeze-dry method shows only one ^{31}P NMR singlet at −2.94 ppm (Fig. 3(d) and 4(a)). High-resolution ESI-MS of the solid isolated by freeze-drying revealed profiles assigned to $[PMo_{11}NbO_{40}]^{4-}$ and $H[PMo_{11}NbO_{40}]^{3-}$ (Fig. S2). These results indicate that the desired $[PMo_{11}NbO_{40}]^{4-}$ can be isolated in a pure form by freeze-drying method.

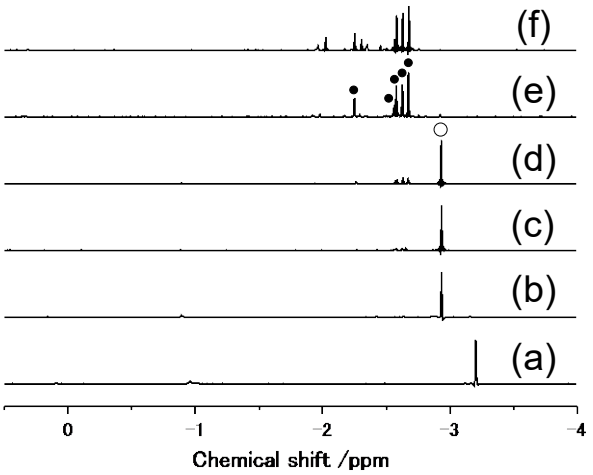

Fig. 2 ^{31}P NMR spectra of (a) $H_3PMo_{12}O_{40}$ (0.15 M), and reaction mixture of $H_3PMo_{12}O_{40}$ (0.15 M) with (b) 1 equivalent, (c) 2 equivalent, (d) 3 equivalent, (e) 4 equivalent, and (f) 5 equivalent of Nb ($K_8Nb_6O_{19}$) in H_2O-D_2O (50 vol%). The reaction mixture was heated at 85 °C for 3 h, and the precipitate formed were removed by centrifugation. An open circle and five closed circles indicate peaks assigned to $[PMo_{11}NbO_{40}]^{4-}$ and $[PMo_{10}Nb_2O_{40}]^{6-}$, respectively.

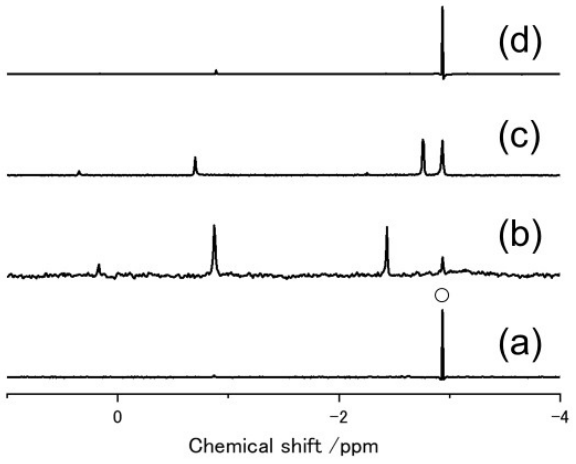

Fig. 3 ^{31}P NMR spectra of (a) aqueous solution containing $[PMo_{11}NbO_{40}]^{4-}$, and solid obtained by drying (b) at 70 °C, (c) at 40 °C, and (d) freeze-drying of the aqueous solution containing $[PMo_{11}NbO_{40}]^{4-}$. Solid (~30 mg) was dissolved with D_2O (~1 mL).

The IR spectrum of the isolated solid showed characteristic bands of Keggin-type phosphomolybdate (Fig. 5), indicating that the isolated solid had a Keggin-type phosphomolybdate structure. The band at ~1094 cm^{-1} corresponding to P-O vibration becomes broader in the case of $[PMo_{11}NbO_{40}]^{4-}$. To comprehend the experimentally observed small differences between the IR spectra of the $[PMo_{12}O_{40}]^{3-}$ and $[PMo_{11}NbO_{40}]^{4-}$ anions, a vibrational frequency analysis was performed for these two species using density-functional theory (DFT). A complete presentation of calculated absorption bands in the 1200–700 cm^{-1} range is given in Fig. S3. The simulated spectra show little change in the position and shape of the asymmetric P-O/Mo=Ot combination band and the M–O–Mo bridging oxygen band. The calculations indicated that the band numbers increased owing to the reduced degenerate normal modes of vibration caused by the substitution of Nb. For example, the band at ~1050 cm^{-1} indicating the P-O vibration became broader, as observed in the experiment. Particularly, a new band at 933 cm^{-1} is attributed to the Nb-Ot band, which may have been observed at ~918 cm^{-1} as a week band in experiment. Elemental analysis of the isolated solid revealed a K:P:Mo:Nb atomic ratio of 1:1:11:1, indicating that the isolated solid was $H_3K[PMo_{11}NbO_{40}]$.

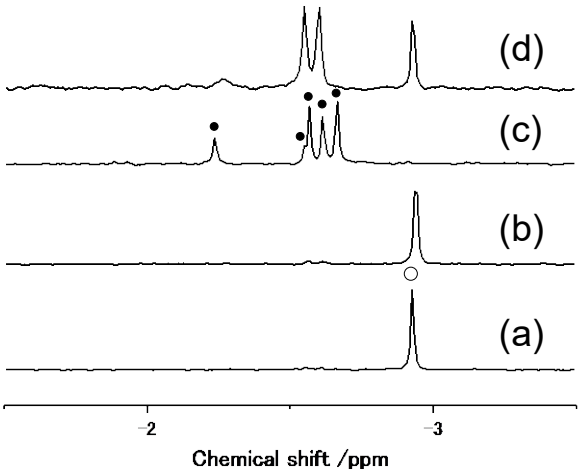

Fig. 4 ^{31}P NMR spectra of (a) solid obtained after freeze-drying the solution of the reaction mixture containing $H_3[PMo_{12}O_{40}]$ and $K_8Nb_6O_{19}$ with Nb/Mo ratio of 1 and subsequent centrifugation ($H_3K[PMo_{11}NbO_{40}]$), (b) solid obtained after freeze-drying of solution which was passed through H+-resin aqueous solution of $H_3K[PMo_{11}NbO_{40}]$, ($H_4[PMo_{11}NbO_{40}]$), (c) solid obtained after freeze-drying of solution of the reaction mixture of $H_3[PMo_{12}O_{40}]$ and $K_8Nb_6O_{19}$ with Nb/Mo ratio of 4 and subsequent centrifugation ($K_5[PMo_{10}Nb_2O_{40}]$), (d) solid obtained after freeze-drying of solution which was passed through H^+-resin of aqueous solution of $K_5[PMo_{10}Nb_2O_{40}]$. Solid (~30 mg) was dissolved with D_2O (~1 mL).

Reaction between $H_3[PMo_{12}O_{40}]$ and $K_8[Nb_6O_{19}]$ can be written as shown in Equation 1. Under our reaction condition, only the desired product, $H_3K[PMo_{11}NbO_{40}]$, is soluble and Mo-based compounds such as $K_2[Mo_6O_{19}]$ are insoluble in the solvent and the desired product could be isolated by centrifugation in pure form. We are not yet able to identify the side products.

$H_3[PMo_{12}O_{40}] + 1/6\ K_8[Nb_6O_{19}] \rightarrow$
$H_3K[PMo_{11}NbO_{40}] + 1/6\ K_2[Mo_6O_{19}]$ (and/or other molybdates) (Equation 1)

The freeze-drying method is suitable for the isolation of all the produced species with different Nb/Mo ratios in aqueous solution, and almost same ^{31}P NMR spectra were observed after freeze-drying (Fig. 4 and S4).

The $[PMo_{11}NbO_{40}]^{4-}$ species were prepared by the reaction of $H_3[PMo_{12}O_{40}]$ and ammonium niobium oxalate, $(NH_4)[NbO(C_2O_4)_2(H_2O)]$, under the same reaction conditions, as confirmed by ^{31}P NMR and high-resolution ESI-MS. However, the elemental analysis of the isolated solid after freeze-drying indicated that the chemical formula was $H_3Nb(C_2O_4)H[PMo_{11}NbO_{40}]$, in which Nb existed as a counter cation.

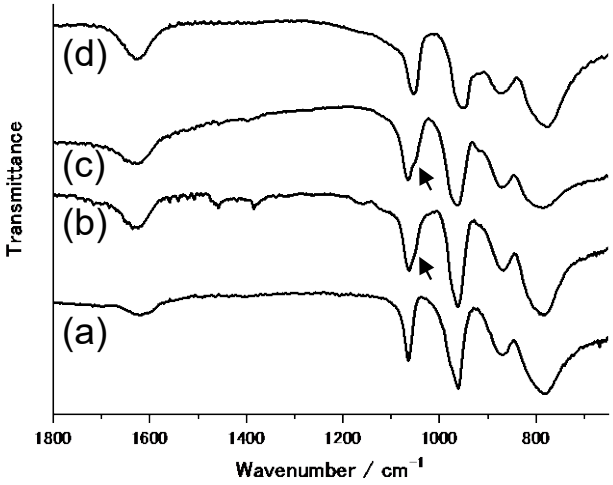

Fig. 5 IR spectra of (a) $H_3[PMo_{12}O40]$, (b) $H_3K[PMo_{11}NbO_{40}]$, (c) $H_4[PMo_{11}NbO_{40}]$, (d) $K_5[PMo_{10}Nb_2O_{40}]$.

The Nb/Mo ratio in the reaction mixture of $H_4[PMo_{12}O_{40}]$ and $K_8[Nb_6O_{19}]$ was varied and then heated at 85 °C for 3 h. ^{31}P NMR spectrum (Fig. 2 (c)-(f)) of the reaction mixture indicated that increasing the Nb/Mo ratio from 1 produced 5 new singlets at −2.68, −2.63, −2.58. −2.57, and −2.25, ppm which corresponds to the di-Nb substituted species, $[PMo_{10}Nb_2O_{40}]^{5-}$ as ^{31}P NMR of $K_5[PMo_{10}Nb_2O_{40}]$ isolated by Weinstock et al. shows similar signals.[27] Similar ^{31}P NMR spectra were obtained after freeze-drying (Fig. 4(c) and S4). When the Nb/Mo ratio was 4, the purity of the di-Nb substituted species, $[PMo_{10}Nb_2O_{40}]^{5-}$ was highest. Elemental analysis of the isolated solid revealed that K:P:Mo:Nb atomic ratio is 5:1:10:2, indicating that the isolated solid was $K_5[PMo_{10}Nb_2O_{40}]$. The chemical formula was same as that of the di-Nb-substituted compound produced by the reaction of Na_2HPO_4, Na_2MoO_4, and $K_8Nb_6O_{19}$ in an acidic solution, followed by the addition of KCl, as reported by Weinstock et al.[27] The IR spectrum of the isolated $K_5[PMo_{10}Nb_2O_{40}]$ showed characteristic bands of Keggin-type structure (Fig. 5(d)), indicating that the isolated solid had a Keggin-type structure.

When the Nb/Mo ratio was greater than 5, additional peaks were observed (Fig. 2(f)). These peaks can be assigned to the tri-Nb substituted species. However, this compound could not be isolated.

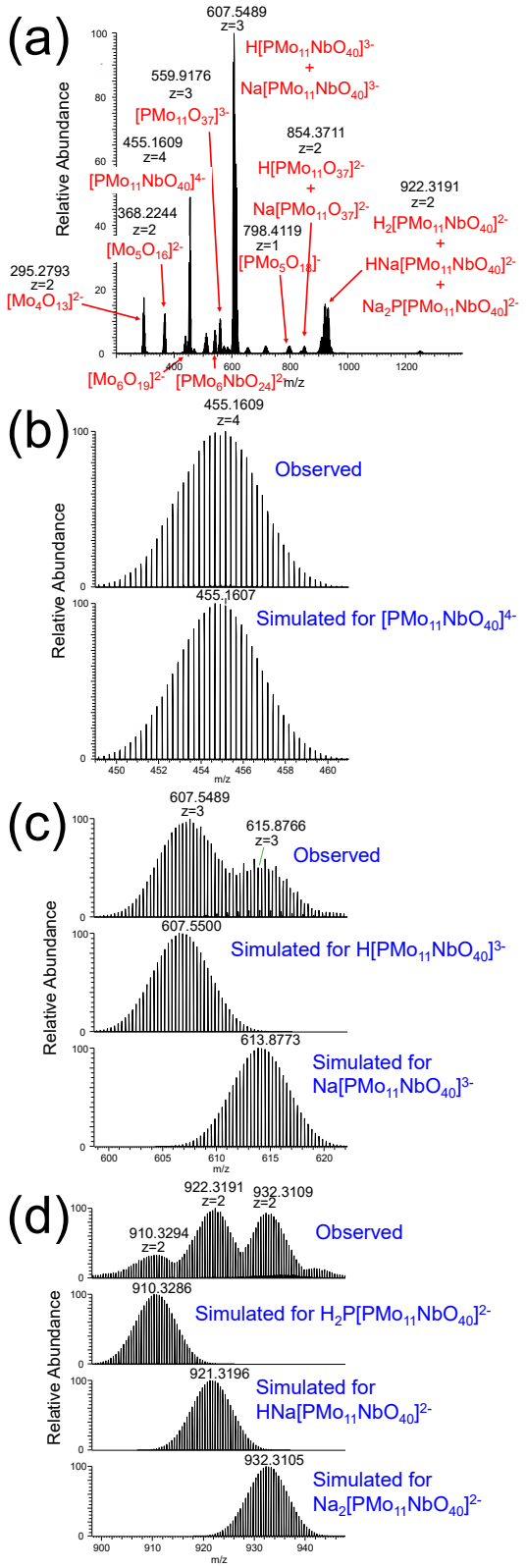

Fig. 6 High-resolution ESI-MS spectra of reaction mixture of H4PMo11NbO40. The solution was diluted by acetonitrile. (a) m/z = 200–1400, (b) enlarged figures m/z = 449–461 together with simulated profile of $[PMo_{11}NbO_{40}]^{4-}$, (c) enlarged figures m/z = 559–622 together with simulated profile of $H[PMo_{11}NbO_{40}]^{3-}$ and $Na[PMo_{11}NbO_{40}]^{3-}$, and (d) enlarged figures m/z = 888–948 together with simulated profile of $H_2[PMo_{11}NbO_{40}]^{2-}$, $HNa[PMo_{11}NbO_{40}]^{2-}$, and $Na_2[PMo_{11}NbO_{40}]^{2-}$.

Isolation of the acidic form

To isolate the pure acidic species, the $H_3K[PMo_{11}NbO_{40}]$ solution obtained after centrifugation was passed through H-resin, and the obtained eluent was freeze-dried. ^{31}P NMR spectra of the isolated species showed one singlet with almost same chemical shift as that of $H_3K[PMo_{11}NbO_{40}]$ (Fig. 4). The IR spectrum of the isolated solid was similar to that of $H_3K[PMo_{11}NbO_{40}]$ (Fig. 5), and the high-resolution ESI-MS spectrum of the isolated solid showed peaks corresponding to $[PMo_{11}NbO_{40}]^{4-}$, $[HPMo_{11}NbO_{40}]^{3-}$, and $[H_2PMo_{11}NbO_{40}]^{2-}$ (Fig. 6), indicating that the Keggin structure was stable under acidic conditions with H-resin. Elemental analysis indicated that the atomic ratio of K:P:Mo:Nb was 0:1:11:1, suggesting that the chemical formula of the isolated solid was $H_4[PMo_{11}NbO_{40}]$.

By contrast, the solid obtained by passing the $K_5[PMo_{10}Nb_2O_{40}]$ solution through the H-resin and subsequent freeze-drying exhibited different ^{31}P NMR peaks (Fig. 4 (d)). ^{31}P NMR of the di-Nbsubstituted species, $K_5[PMo_{10}Nb_2O_{40}]$, with different HCl concentrations (Fig. S5) indicates that the $[PMo_{10}Nb_2O_{40}]^{5-}$ decomposes by decreasing pH.

Thermal stability of $H_4[PMo_{11}NbO_{40}]$

The TG-DTA profile of the isolated $H_4[PMo_{11}NbO_{40}]$ (Fig. 7) shows a gradual weight loss. Ressler et al. reported that $H_4[PMo_{11}NbO_{40}]$ shows an endothermal signal at approximately 300 °C,[23] but we did not observe such endothermal peak. Isolated $H_4[PMo_{11}NbO_{40}]$ was heated in air at different temperatures (temperature was raised at 10 °C/min, and the temperature was kept for 1 h), and the obtained solids were characterized by ^{31}P NMR (Fig. 8), IR (Fig. 9), and powder X-Ray diffraction (XRD; Fig. 10). When the $H_4[PMo_{11}NbO_{40}]$ is heated at 100 °C, a small new ^{31}P NMR peak at −0.86 ppm appeared, and the intensity of the peak increases by increasing temperature. When the temperature is more than 300 °C, additional peaks between −0.4 and −0.6 ppm appeared. However, signal assignable to $[PMo_{11}NbO_{40}]^{4-}$is the main peak up to 350 °C. When the temperature was increased to 400 °C, the peak assignable to $[PMo_{11}NbO_{40}]^{4-}$ disappeared. The IR spectra of the heated samples indicated similar thermal behaviours. The characteristic bands for $[PMo_{11}NbO_{40}]^{4-}$ are observed as the main bands until 350 °C, but new bands are observed after heating at 200 °C, and the bands intensities increased by increasing the temperature. The powder XRD patterns of the heated samples indicate that heating at 400 °C produces Mo-Nb-based oxides[38] and further heating at 500 °C produces mostly MoO_3.

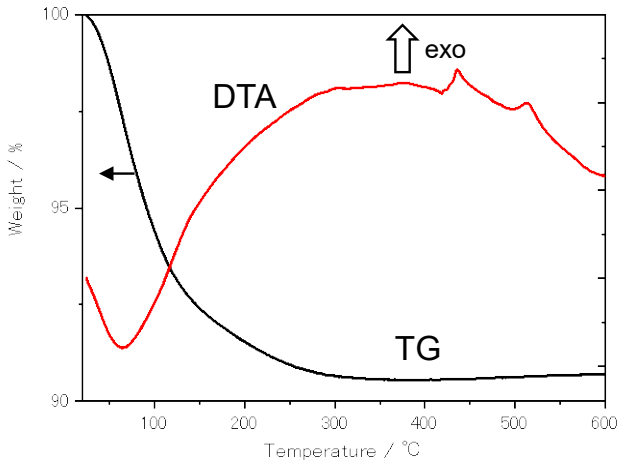

Fig. 7 TG-DTA curves of $H_4[PMo_{11}NbO_{40}]$ in N_2 flow (50 mL min^{-1}).

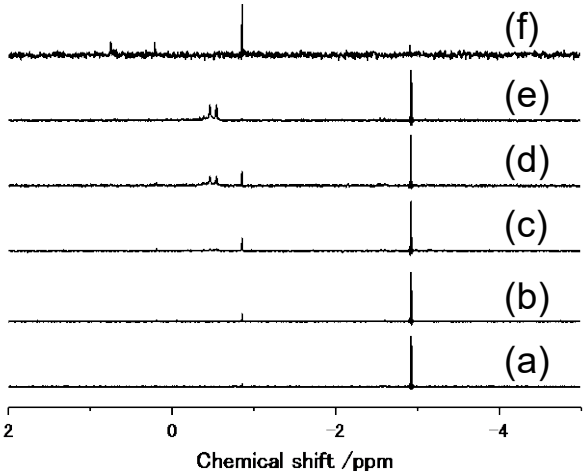

Fig. 8 ^{31}P NMR spectra of $H_4[PMo_{11}NbO_{40}]$ after heating at different heating temperatures. (a) without heating, (b) 100, (c) 200, (d) 300, (e) 350 and (f) 400 °C. Solid (~30 mg) was dissolved with D_2O (~1 mL).

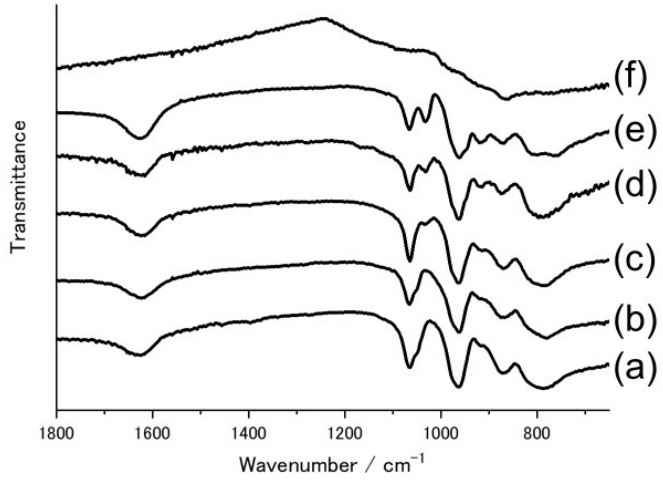

Fig. 9 IR spectra of $H_4[PMo_{11}NbO_{40}]$ after heating at different heating temperatures. (a) without heating, (b) 100, (c) 200, (d) 300, (e) 350 and (f) 400 °C.

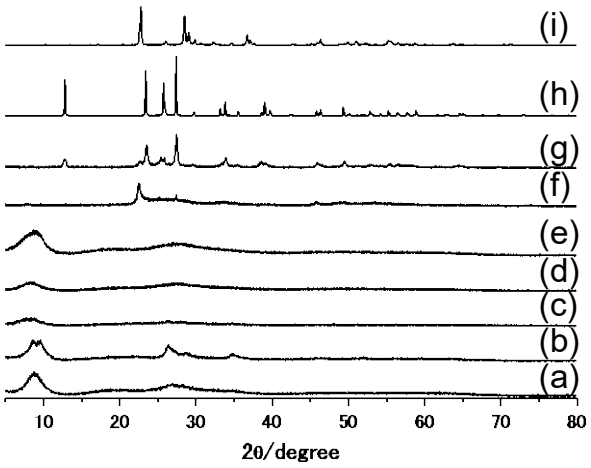

Fig. 10 Powder XRD spectra of $H_4[PMo_{11}NbO_{40}]$ after heating at different heating conditions. (a) without heating, (b) 100, (c) 200, (d) 300, (e) 350, (f) 400 and (g) 500 °C. Powder XRD of (h) MoO_3 and (i) Nb_2O_5.

The $H_4[PMo_{11}NbO_{40}]$ was the main species after heating at 350 °C under out heating condition, although drying the aqueous solution of $H_4[PMo_{11}NbO_{40}]$ at 40 °C decomposed the $H_4[PMo_{11}NbO_{40}]$ molecule (Fig. 3 (c)). The decomposition of $H_4[PMo_{11}NbO_{40}]$ occurred more rapidly in aqueous solution. We believe there is an equilibrium between $[PMo_{11}NbO_{40}]^{4-}$ and other molybdate derivatives in aqueous solution, and drying from solution easily decomposed $[PMo_{11}NbO_{40}]^{4-}$. On the other hand, removal of H_2O from ice by freeze-drying method hindered decomposition.

Redox properties of $H_4[PMo_{11}NbO_{40}]$

Cyclic voltammetry (CV) result of $H_4[PMo_{11}NbO_{40}]$ was compared with that of $H_3[PMo_{12}O_{40}]$, $H_4[SiMo_{12}O_{40}]$, and $H_4[PMo_{11}VO_{40}]$ in 0.1 M H_2SO_4 in a H_2O-1,4-dioxane (1:1 vol) solution (Fig. 11), where well-defined reversible redox couples of $H_3[PMo_{12}O_{40}]$ were obtained. It has been reported that $H_3[PMo_{12}O_{40}]$ is unstable in water; however, its stability increases with the addition of an organic cosolvent,[39] and $H_3[PMo_{12}O_{40}]$ and $H_4[SiMo_{12}O_{40}]$ exhibit well-defined three 2-electron redox couples in mixed solvent system. $H_4[PMo_{11}NbO_{40}]$ exhibited three well-defined redox couples that can be assigned to three 2-electron redox processes by comparing the peak currents with those of $H_3[PMo_{12}O_{40}]$ and $H_4[SiMo_{12}O_{40}]$. For $H_4[PMo_{11}VO_{40}]$, a one-electron redox reaction of $V^{5+/4+}$ was observed at ~500 mV. However, no redox couple corresponding to $Nb^{5+/4+}$ was observed. These results indicated that $H_4[PMo_{11}NbO_{40}]$ shows three 2-electron reduction couples for Mo. The three reduction potentials were more negative than those of $H_3[PMo_{12}O_{40}]$. This can be explained by the difference in negative charges. More negative $[PMo_{11}NbO_{40}]^{4-}$ needs more reduction potentials compared to $[PMo_{12}O_{40}]^{3-}$.

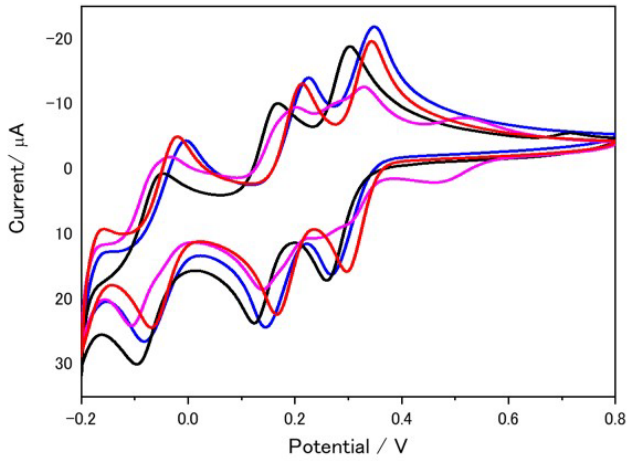

Fig. 11 Cyclic voltammogram of (black line) $H_4[PMo_{11}NbO_{40}]$, (red line) $H_3[PMo_{12}O_{40}]$, (blue line) $H_4[SiMo_{12}O_{40}]$ and (pink line) $H_4[PMo_{11}VO_{40}]$ in 0.1 M H_2SO_4 in H_2O-1,4-Dioxane (1:1 vol) solution. Concentration of all complexes was 1 mM.

Catalytic performance of oxidative dehydrogenation of isobutylaldehyde to methacrolein

Oxidative dydrogenation of isobutylaldehyde using O_2 as an oxidant is one of the important methods to produce methacrolein, an important feedstock for polymers, and salts of Keggin-type phosphomolybdic acids have been utilized as catalysts. The catalytic performances of $H_4[PMo_{11}NbO_{40}]$, $H_4[PMo_{11}VO_{40}]$ and $H_3[PMo_{12}O_{40}]$ were evaluated for heterogeneous oxidative dehydrogenation of isobutylaldehyde using O_2 as an oxidant (Table 1).[37] Isobutylaldehyde conversions and methacrolein yields were plotted against gas-space velocities ($W{\cdot}F^{-1}$) where W and F represent the catalyst mass (kg) and the flow rate of isobutylaldehyde (m^3/s), respectively, in Fig. 12. All catalysts produced the desired methacrolein as the main product, together with CO/CO_2 as byproducts. Among them, $H_4[PMo_{11}NbO_{40}]$ showed the highest isobutylaldehyde conversion and methacrolein yield. Reaction rates were estimated to be 6.3×10^{-3}, 4.3×10^{-3}, and 3.0×10^{-3} $m^3{\cdot}kg^{-1}{\cdot}s^{-1}$, for $H_4[PMo_{11}NbO_{40}]$, $H_4[PMo_{11}VO_{40}]$, and $H_3[PMo_{12}O_{40}]$, respectively, assuming isobutylaldehyde conversation as the first order reaction. The reaction rate constant of $H_4[PMo_{11}NbO_{40}]$ was twice that of $H_3[PMo_{12}O_{40}]$. Further investigations into why $H_4[PMo_{11}NbO_{40}]$ showed better performance than $H_4[PMo_{11}VO_{40}]$ and $H_3[PMo_{12}O_{40}]$ are ongoing by our group.

Table 1 Heterogeneous oxidation of isobutyraldehyde.

No	Catalyst	$W{\cdot}F^{-1}$ [$kg{\cdot}s{\cdot}m^{-3}$]	Isobutyl-aldehyde Conv. [%]	Methacrolein Yield [%]	Sel. [%]
1	$H_4[PMo_{11}NbO_{40}]$	313.1	84.1	78.8	93.7
2	$H_4[PMo_{11}NbO_{40}]$	442.1	94.1	88.4	93.9
3	$H_4[PMo_{11}VO_{40}]$	223.5	63.6	55.3	87.7
4	$H_4[PMo_{11}VO_{40}]$	452.4	83.8	75.3	75.3
5	$H_3[PMo_{12}O_{40}]$	230.0	44.7	37.3	83.3
6	$H_3[PMo_{12}O_{40}]$	441.2	77.9	69.4	89.1
7	$H_3[PMo_{12}O_{40}]$	672.5	83.1	74.1	89.1

Reaction gas containing isobutylaldehyde, O_2, H_2O, and N_2 with partial pressure of 1.4, 10.1, 10.3, and 78.5 kPa, respectively, was passed through catalysts fixed in a fixed-bed continuous flow reactor under atmospheric pressure at 240 °C.

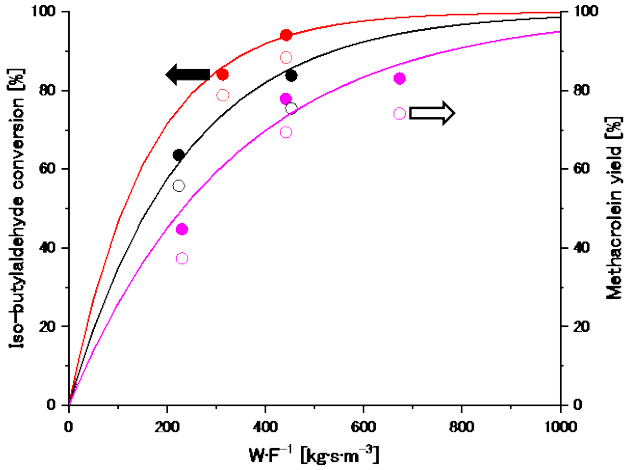

Fig. 12 Isobutylaldehyde conversion (closed circles), conversion curves (lines) estimated by assumption that the conversion is first-order with respect to isobutylaldehyde concentration, methacrolein yields (open circles) against gas-space velocities ($W{\cdot}F^{-1}$) using $H_4[PMo_{11}NbO_{40}]$ (red), $H_4[PMo_{11}VO_{40}]$ (black), and $H_4[PMo_{12}O_{40}]$ (pink).

Catalytic performance of Wacker-type oxidation of allyl phenyl ether to methyl ketone

Wacker-type reactions are useful method to convert olefins to carbonyl compounds using Pd^{2+} and Cu^{2+} as catalysts and O_2 as an oxidant. In Wacker-type reactions,[9] olefins activated by coordination to Pd^{2+} react with water molecules to produce carbonyl compounds and Pd^0 intermediates. The Pd^0 species is re-oxidized by Cu^{2+} to form Pd^{2+} and Cu^+, and the Cu^+ is oxidized to Cu^{2+} by molecular O_2. It has been known that Keggin-type phosphomolybdic acid derivatives are alternatives of Cu^{2+} to re-generate active Pd^{2+} catalysts.[9] Recently, Hong et al. reported that a mixture of $Pd(OAc)_2$ and $H_3PMo_{12}O_{40}$ or $H_4PMo_{11}VO_{40}$ showed good catalytic activity for the Wacker-type oxidation of allyl phenyl ether, forming phenoxyacetone and phenoxypropane-1-al as Wacker-oxidation products and phenol as a by-product (Equation 2, Table 2).[40] We performed the reaction at 60 °C in the presence of 10 mol% $Pd(OAc)_2$ and 3 mol% POMs with a balloon filled with O_2 gas under the same conditions reported by Hong et al.

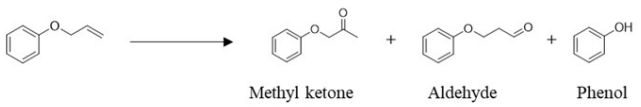

(Equation 2)

Table 2 Wacker-type oxidation of allylphenyll ether

No	POMs	Conv. [%]	Yield [%]		
		Allylphenyl ether	Methyl ketone	Aldehyde	Phenol
1	$H_4[PMo_{11}NbO_{40}]$	77	42	10	25
2	$H_4[PMo_{11}VO_{40}]$	98 (100)[a]	67 (65)[a]	6 (12)[a]	25 (14)[a]
3	$H_3[PMo_{12}O_{40}]$	47 (41)[a]	18 (23)[a]	2 (6)[a]	27 (6)[a]

Conditions: $Pd(OAC)_2$ (10 mol%), POMs (3 mol%), and Acetonitrile/H_2O (7/1 (v/v)) at 60 °C for 18 h. a) Values in parentheses are reported in Ref. 31.

The reactions with $H_3[PMo_{12}O_{40}]$ and $H_4[PMo_{11}NbO_{40}]$ showed similar conversions and yields to those reported by the Hong group, where the activity of $H_4[PMo_{11}VO_{40}]$ exhibited better performance (Table 2, No. 2 and 3). The catalytic activity of $H_4[PMo_{11}NbO_{40}]$ (Table 2, No. 1) was intermediate between those of $H_3[PMo_{12}O_{40}]$ and $H_4[PMo_{11}VO_{40}]$. The first reversible reduction potentials of $H_4[PMo_{11}NbO_{40}]$, $H_3[PMo_{12}O_{40}]$, and $H_4[PMo_{11}VO_{40}]$, estimated by CV, were 280, 320, and 500 mV, respectively, which may influence Pd^0 oxidation and re-oxidation of the reduced polyoxomolybdates by O_2. We have no clear explanation to explain activity differences using only redox potential differences. ^{31}P NMR of $H_4[PMo_{11}VO_{40}]$ in aqueous solution showed several peaks (Fig. S6) indicating that $H_4[PMo_{11}VO_{40}]$ contains several impurities. Some of the impurities might be catalytic active species. We are currently conducting further investigations to explain these differences in performance.

Conclusions

Mono-Nb substituted Keggin-type phosphomolybdate, $[PMo_{11}NbO_{40}]^{4-}$, was prepared by mixing Keggin-type phosphomolybdic acid, $H_3[PMo_{12}O_{40}]$, and potassium hexaniobate, $K_8Nb_6O_{19}$, and subsequent centrifugation in water. The potassium and proton mixed salt, $KH_3[PMo_{11}NbO_{40}]$, was isolated by freeze-drying the reaction mixture, and all the protonic forms, $H_4[PMo_{11}NbO_{40}]$, were isolated by proton exchange with H-resin and subsequent freeze-drying. The isolated $H_4[PMo_{11}NbO_{40}]$ was thermally stable up to ~350 °C in air and could be used as heterogeneous catalyst for isobutylaldehyde using O_2 as an oxidant. Furthermore, $H_4[PMo_{11}NbO_{40}]$ exhibited catalytic activity for Wacker-type oxidation.

Author Contributions

T. Matono, N. Umehara, T. Sano and M. Sadakane synthesized and characterized POMs. S. Ueno, Y. Kato, W. Ninomiya, M. E. Hallal, E. O. Y. Gonzales, M. Capron, S. Ishikawa and W. Ueda performed catalytic tests. Z. Lang and Y. Li performed DFT calculations. M. Sadakane organized the whole researches.

Conflicts of interest

There are no conflicts to declare.

Acknowledgements

This work was supported by Grant-in-Aid for Transformative Research Area (A) “Supra-ceramics” (JSPS KAKENHI Grant Number JP22H05144), JSPS Core-to-Core Program, International Associated Laboratory (LIA) “Nano oxide-based catalysts for biomass valorization (NANOXCAT),” and International Network on Polyoxometalate Science at Hiroshima University. We thank Ms. T Amimoto at the Natural Science Center for Basic Research and Development (N-BARD), Hiroshima University, for ESI-MS measurements.

Notes and references

1. M. T. Pope, *Heteropoly and Isopoly Oxometalates*, Springer-Verlag, Berlin, 1983.
2. C. L. Hill, *Chem. Rev.*, 1998, **98**, 1-390.
3. L. Cronin, *Chem. Soc. Rev.*, 2012, **41**, 7325-7648.
4. S. Ishikawa, T. Ikeda, M. Koutani, S. Yasumura, K. Amakawa, K. Shimoda, Y. Jing, T. Toyao, M. Sadakane, K.-i. Shimizu and W. Ueda, *J. Am. Chem. Soc.*, 2022, **144**, 7693-7708.
5. S. Ogo, M. Miyamoto, Y. Ide, T. Sano and M. Sadakane, *Dalton Trans.*, 2012, **41**, 9901-9907.
6. I. A. Weinstock, R. E. Schreiber and R. Neumann, *Chem. Rev.*, 2018, **118**, 2680-2717.
7. M. Lechner, R. Guttel and C. Streb, *Dalton Trans.*, 2016, **45**, 16716-16726.
8. C. T. Buru, M. C. Wasson and O. K. Farha, *ACS Appl. Nano Mater.*, 2019, **3**, 658-664.
9. J. Muzart, *Tetrahedron*, 2021, **87**, 132024.
10. M. Nyman, *Dalton Trans.*, 2011, **40**, 8049-8058.
11. E. V. Radkov, Y. J. V. G. and R. H. Beer, *J. Am. Chem. Soc.*, 1999, **121**, 8953-8954.
12. E. V. Radkov and R. H. Beer, *Inorg. Chim. Acta*, 2000, **297**, 191-198.
13. E. Cadot, V. Béreau and F. Sécheresse, *Inorg. Chim. Acta*, 1985, **239**, 39-42.
14. E. Radkov and R. H. Beer, *Polyhedron*, 1995, **14**, 2139-2143.
15. K. Okumura, K. Yamashita, K. Yamada and M. Niwa, *J. Catal.*, 2007, **245**, 75-83.
16. D. R. Park, S. Park, Y. Bang and I. K. Song, *Appl. Catal. A. Gen.*, 2010, **373**, 201-207.
17. P. A. Abramov, A. Shmakova, M. Haouas, G. Fink, E. Cadot and M. N. Sokolov, *New J. Chem.*, 2017, **41**, 256-262.
18. A. A. Shmakova, M. M. Akhmetova, V. V. Volchek, T. E. Romanova, I. Korolkov, D. G. Sheven, S. A. Adonin, P. A. Abramov and M. N. Sokolov, *New J. Chem.*, 2018, **42**, 7940-7948.
19. M. Pohl and R. G. Finke, *Organometallics*, 1993, **12**, 1453-1457.
20. M. Alizadeh and B. Yadollahi, *New J. Chem.*, 2022, **46**, 18199-18206.

21. N. V. Maksimchuk, G. Maksimov, V. Y. Evtushok, I. D. Ivanchikova, Y. A. Chesalov, R. I. Maksimovskaya, O. A. Kholdeeva, A. Solé-Daura, J. M. Poblet and J. J. Carbó, *ACS Catal.*, 2018, **8**, 9722-9737.
22. O. V. Zalomaeva, N. V. Maksimchuk, G. Maksimov and O. A. Kholdeeva, *Eur. J. Inorg. Chem.*, 2019, 410-416.
23. T. Ressler, O. Timpe and F. Girgsdies, *Z. Kristallogr.*, 2005, **220**, 295-305.
24. J. H. Holles, C. J. Dillon, J. A. Labinger and M. E. Davis, *J. Catal.*, 2003, **218**, 42-53.
25. C. J. Dillon, J. H. Holles, R. J. Davis, J. A. Labinger and M. E. Davis, *J. Catal.*, 2003, **218**, 54-66.
26. P. A. Abramov, T. E. Romanova, V. V. Volchek, A. A. Mukhacheva, N. B. Kompankov and M. N. Sokolov, *New J. Chem.*, 2018, **42**, 7949-7955.
27. G. Zhang, E. Gadot, G. Gan-Or, M. Baranov, T. Tubul, A. Neyman, M. Li, A. Clotet, J. M. Poblet, P. Yin and I. A. Weinstock, *J. Am. Chem. Soc.*, 2020, **142**, 7295-7300.
28. A. D. Becke, *J. Chem. Phys.*, 1993, **98**, 5648-5652.
29. W. Y. C. Lee, R. G. Parr, *Phys Rev B Condens Matter*, 1988, **37**, 785-789.
30. M. J. Frisch, G. W. Trucks, H. B. Schlegel, G. E. Scuseria, M. A. Robb, J. R. Cheeseman, G. Scalmani, V. Barone, B. Mennucci, G. A. Petersson, H. Nakatsuji, M. Caricato, X. Li, H. P. Hratchian, A. F. Izmaylov, J. Bloino, G. Zheng, J. L. Sonnenberg, M. Hada, M. Ehara, K. Toyota, R. Fukuda, J. Hasegawa, M. Ishida, T. Nakajima, Y. Honda, O. Kitao, H. Nakai, T. Vreven, J. A. Montgomery Jr., J. E. Peralta, F. Ogliaro, M. J. Bearpark, J. J. Heyd, E. N. Brothers, J. A. Montgomery Jr., J. E. Peralta, F. Ogliaro, M. J. Bearpark, J. J. Heyd, E. N. Brothers, J. A. Montgomery Jr., J. E. Peralta, F. Ogliaro, M. J. Bearpark, J. J. Heyd, E. N. Brothers, K. N. Kudin, V. N. Staroverov, T. A. Keith, R. Kobayashi, J. Normand, K. Raghavachari, A. P. Rendell, J. C. Burant, S. S. Iyengar, J. Tomasi, M. Cossi, N. Rega, J. M. Millam, M. Klene, K. J. E., C. J. B., B. V., C. Adamo, J. J., R. Gomperts, R. E. Stratmann, O. Yazyev, A. J. Austin, R. Cammi, C. Pomelli, J. W. Ochterski, R. L. Martin, K. Morokuma, V. G. Zakrzewski, G. A. Voth, P. Salvador, J. J. Dannenberg, S. Dapprich, A. D. Daniels, O. Farkas, J. B. Foresman, J. V. Ortiz, J. Cioslowski and D. J. Fox, Gaussian 09 Rev. D.01, Wallingford, CT, 2013.
31. G. S. C. A. D. McLean, *J. Chem. Phys.*, 1980, **72**, 5639-5648.
32. J. S. B. R. Krishnan, R. Seeger, J. A. Pople, *J. Chem. Phys.*, 1980, **72**, 650-654.
33. P. F. L. V. Szentpaly, H. Preuss, H. Stoll, *Chem. Phys. Lett.*, 1982, **93**, 555.
34. M. D. X. Cao, *J. Chem. Phys.*, 2001, **115**, 7348.
35. H. S. M. Dolg, H. Preuss, *Theor. Chim. Acta*, 1993, **85**, 441.
36. H. S. M. Dolg, H.-J. Flad, H. Preuss, *J. Chem. Phys.*, 1992, **97**, 1162-1173.
37. J. B. P. Čičmaneč, J. Tichý, *React. Kinet. Catal. Lett.*, 2004, **81**, 383-391.
38. T. Murayama, N. Kuramata, S. Takatama, K. Nakatani, S. Izumi, X. Yi and W. Ueda, *Catal. Today*, 2012, **185**, 224-229.
39. M. Sadakane and E. Steckhan, *Chem. Rev.*, 1998, **98**, 219-237.
40. S. Tamura, Y. Shimoyama, D. Hong and Y. Kon, *Mol. Catal.*, 2020, **496**, 111178.

Supplementary Material

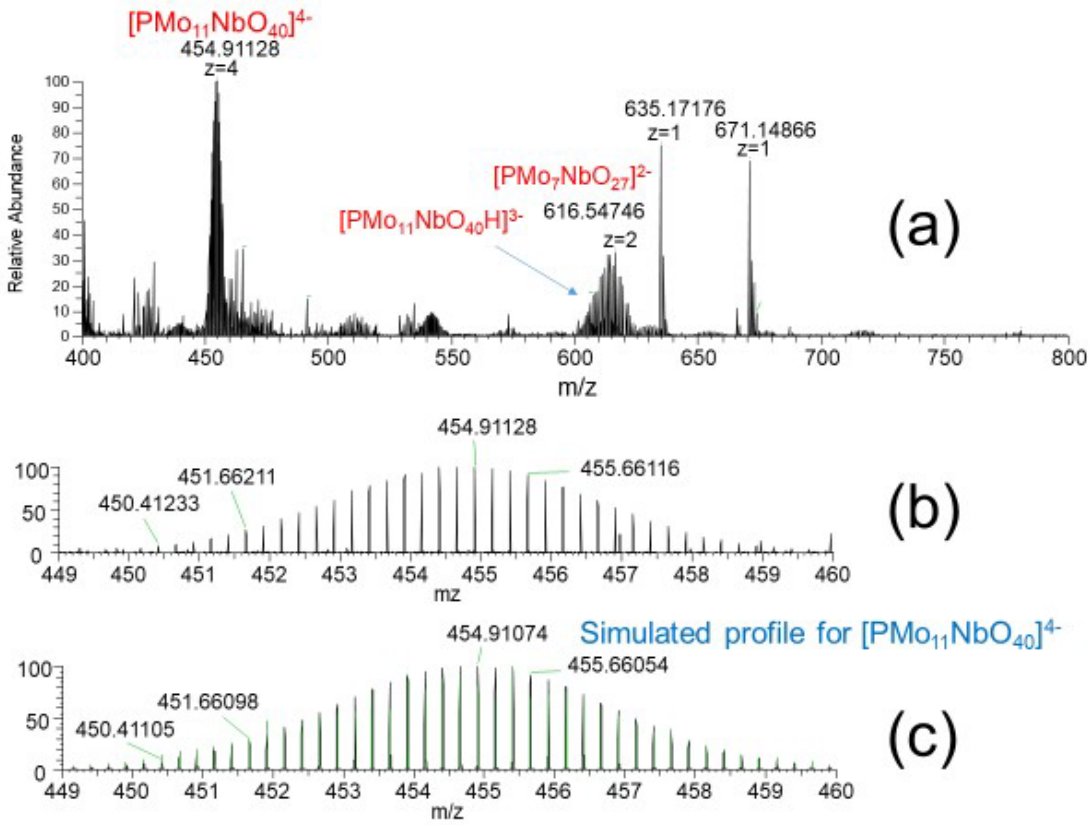

Figure S1. High-resolution ESI-MS spectra of reaction mixture of $H_3PMo_{12}O_{40}$ and $K_8Nb_6O_{19}$ (1 equivalent of Nb to $H_3PMo_{12}O_{40}$) which was heated at 85 ºC for 3 h followed by centrifugation. The resulting solution was then dissolved in acetonitrile. (a) m/z = 400–800. (b) Enlarged m/z = 449–460, and (c) simulated profile of $[PMo_{11}NbO_{40}]^{4-}$.

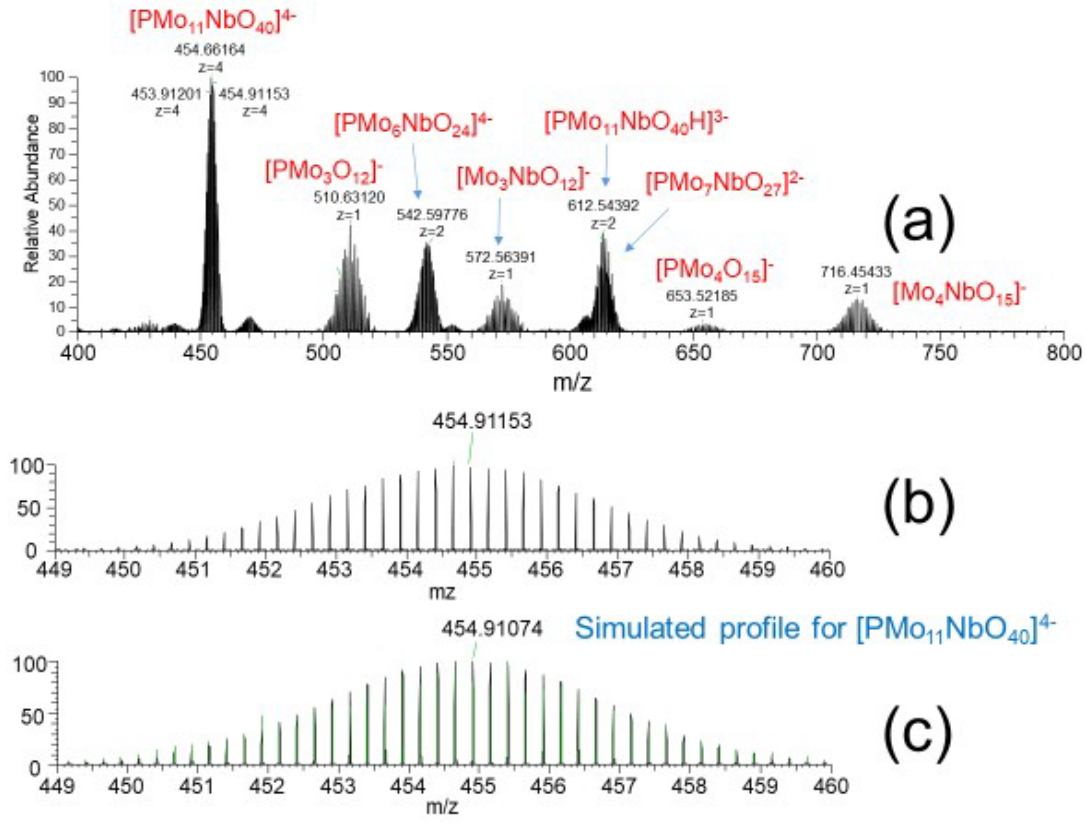

Figure S2. High-resolution ESI-MS spectra of the solid obtained by freeze-drying a solution of $H_3KPMo_{11}NbO_{40}$ dissolved in acetonitrile. (a) m/z = 400–800. (b) Enlarged m/z = 449–460, and (c) simulated profile of $[PMo_{11}NbO_{40}]^{4-}$.

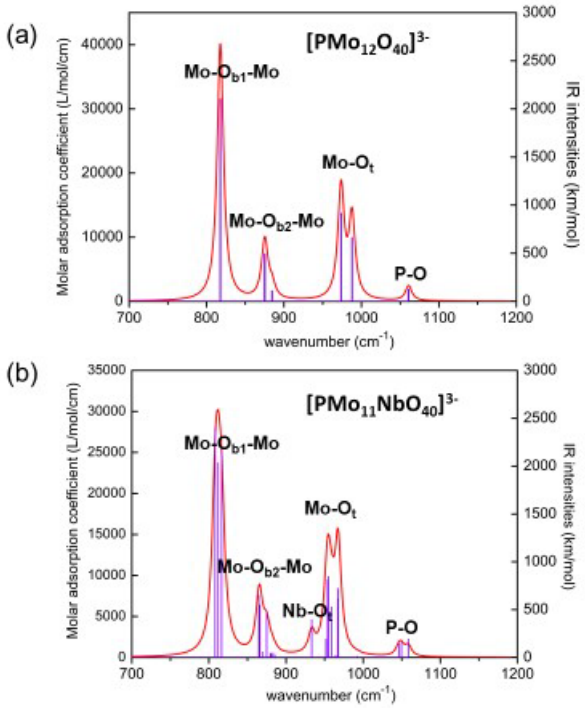

Figure S3. Simulated IR spectra of (a) $[PMo_{12}O_{40}]^{3-}$ and (b) $[PMo_{11}NbO_{40}]^{4-}$ at the B3LYP/6+31+G(d, p)/SDD level.

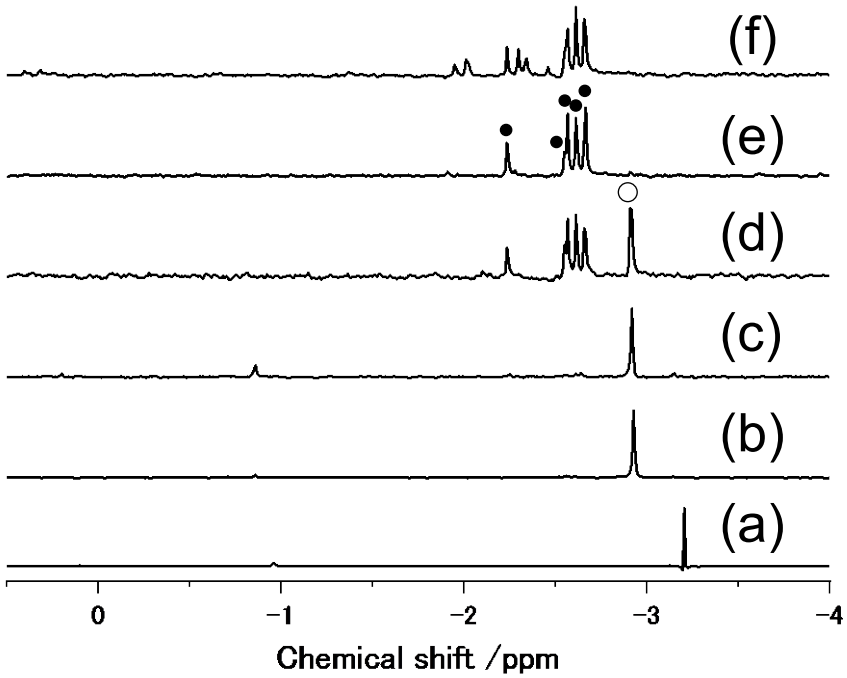

Figure S4. ^{31}P NMR spectra of (a) $H_3PMo_{12}O_{40}$ (0.15 M) and the solid obtained after freeze-drying the reaction mixture of $H_3PMo_{12}O_{40}$ (0.15 M) with (b) 1, (c) 2, (d) 3, (e) 4, and (f) 5 equiv of Nb ($K_8Nb_6O_{19}$) in H_2O. The reaction mixture was heated at 85 °C for 3 h, and the precipitate was removed by centrifugation. The open circles and five closed circles indicate peaks assignable to $[PMo_{11}NbO40]^{4-}$ and $[PMo_{10}Nb_2O_{40}]^{6-}$, respectively. The solid (~30 mg) was dissolved in D_2O (~1 mL).

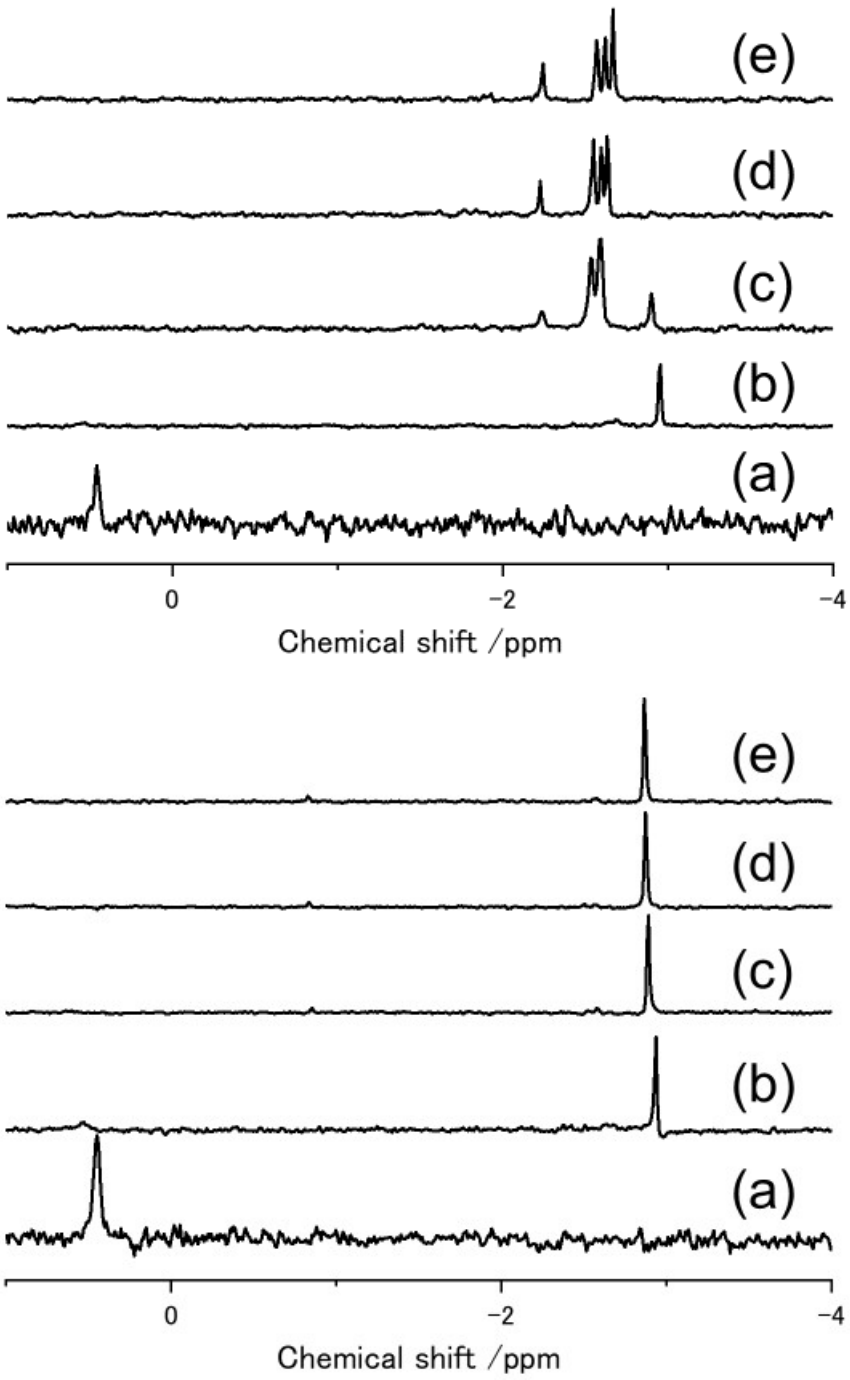

Figure S5. ^{31}P NMR spectra of (top) $K_5[PMo_{10}Nb_2O_{40}]$ and (bottom) $H_3K[PMo_{11}NbO_{40}]$ in (a) 6 M HCl, (b) 1.2 M HCl, (c) 0.24 M HCl, (d) 0.048 M HCl, and (e) 0.0096 M HCl aqueous solution.

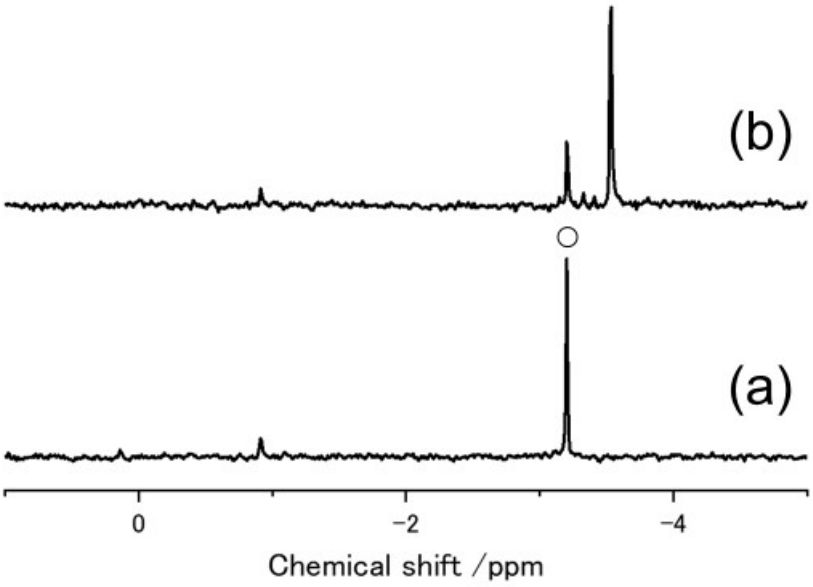

Figure S6. ^{31}P NMR spectra of (a) $H_3[PMo_{12}O_{40}]$ and (b) $H_4[PMo_{11}VO_{40}]$. Solid (~30 mg) was dissolved with D_2O (~1 mL).